ESC European Society of Cardiology

Cardiovascular Research (2018) **114**, 1848–1859
doi:10.1093/cvr/cvy134

Generation and primary characterization of iAM-1, a versatile new line of conditionally immortalized atrial myocytes with preserved cardiomyogenic differentiation capacity

Jia Liu[1,2,3], Linda Volkers[1], Wanchana Jangsangthong[1†], Cindy I. Bart[1], Marc C. Engels[1‡], Guangqian Zhou[2], Martin J. Schalij[1], Dirk L. Ypey[1], Daniël A. Pijnappels[1], and Antoine A.F. de Vries[1,3]*

[1]Laboratory of Experimental Cardiology, Department of Cardiology, Leiden University Medical Center, Albinusdreef 2, 2300 RC Leiden, The Netherlands; [2]Department of Cell Biology and Genetics, Center for Anti-ageing and Regenerative Medicine, Shenzhen Key Laboratory for Anti-ageing and Regenerative Medicine, Shenzhen University Medical School, Shenzhen University, Nanhai Ave 3688, Shenzhen, 518060, China; and [3]Netherlands Heart Institute, Holland Heart House, Moreelsepark 1, 3511 EP, Utrecht, The Netherlands

Received 6 February 2017; revised 30 June 2017; editorial decision 17 May 2018; accepted 13 June 2018; online publish-ahead-of-print 18 June 2018

Time for primary review: 35 days

Aims The generation of homogeneous cardiomyocyte populations from fresh tissue or stem cells is laborious and costly. A potential solution to this problem would be to establish lines of immortalized cardiomyocytes. However, as proliferation and (terminal) differentiation of cardiomyocytes are mutually exclusive processes, their permanent immortalization causes loss of electrical and mechanical functions. We therefore aimed at developing conditionally immortalized atrial myocyte (iAM) lines allowing toggling between proliferative and contractile phenotypes by a single-component change in culture medium composition.

Methods and results Freshly isolated neonatal rat atrial cardiomyocytes (AMs) were transduced with a lentiviral vector conferring doxycycline (dox)-controlled expression of simian virus 40 large T antigen. Under proliferative conditions (i.e. in the presence of dox), the resulting cells lost most cardiomyocyte traits and doubled every 38 h. Under differentiation conditions (i.e. in the absence of dox), the cells stopped dividing and spontaneously reacquired a phenotype very similar to that of primary AMs (pAMs) in gene expression profile, sarcomeric organization, contractile behaviour, electrical properties, and response to ion channel-modulating compounds (as assessed by patch-clamp and optical voltage mapping). Moreover, differentiated iAMs had much narrower action potentials and propagated them at >10-fold higher speeds than the widely used murine atrial HL-1 cells. High-frequency electrical stimulation of confluent monolayers of differentiated iAMs resulted in re-entrant conduction resembling atrial fibrillation, which could be prevented by tertiapin treatment, just like in monolayers of pAMs.

Conclusion Through controlled expansion and differentiation of AMs, large numbers of functional cardiomyocytes were generated with properties superior to the differentiated progeny of existing cardiomyocyte lines. iAMs provide an attractive new model system for studying cardiomyocyte proliferation, differentiation, metabolism, and (electro)-physiology as well as to investigate cardiac diseases and drug responses, without using animals.

Keywords Atrial cardiomyocyte • Conditional immortalization • Large T antigen • Cardiomyogenic differentiation • HL-1 cells

* Corresponding author. Tel: +31-71-5265859; fax: +31-71-5266809, E-mail: a.a.f.de_vries@lumc.nl

† Present address. Institute of Physiology I, University of Bonn, Life and Brain Center, Sigmund-Freud-Strasse 25, 53127 Bonn, Germany.

‡ Present address. Emory University School of Medicine, 100 Woodruff Circle, Suite 327 School of Medicine Building, Atlanta, GA 30303-3073, USA.

Introduction

Due to the limited availability of human heart tissue and the low mitotic activity of postnatal human cardiomyocytes, cardiac research has strongly relied on experiments in animals[1,2] or with primary cardiomyocytes of animal origin.[3,4] The increasing opposition to the use of animals for biomedical research has fuelled the search for alternative models of human cardiac disease.

Recently, cardiomyocytes derived from pluripotent stem cells (PSC-CMCs) have emerged as new models for studying different aspects of cardiac disease. Despite the great potential of PSC-CMCs as cardiac model systems, they have some serious drawbacks that need to be overcome before becoming a practical alternative to the use of laboratory animals. Both the generation of PSCs and the production of homogeneous populations of cardiomyocytes from these cells is a laborious, time-consuming, and costly endeavour of varying efficiency, which requires properly timed treatment of the starting material with different cocktails of expensive growth factors and small molecules.[5] Moreover, PSCs greatly differ in their ability to differentiate into cardiomyocytes and typically yield phenotypically heterogeneous populations of immature cardiac muscle cells.[6,7] The latter feature is limiting the use of PSC-CMCs in studying cardiac physiology and pathology, e.g. it has been proven difficult to establish homogeneous (confluent) monolayers of these cells for cardiac arrhythmia research by high-resolution optical mapping.[8]

As another approach to reduce laboratory animal use in cardiac research, cardiomyocyte lines have been generated using cardiac muscle cells from rodents and humans as starting material and the simian virus 40 (SV40) large T (LT) antigen to induce cell proliferation.[9–15] Unfortunately, all cardiomyocyte lines generated thus far, including the widely used HL-1 cell line, display large structural, and functional deficits in comparison to the primary cells from which they were indirectly derived.

In an attempt to overcome the paucity of cell lines with robust cardiomyogenic differentiation capacity, we developed a new strategy to selectively and conditionally immortalize cardiomyocytes. Given our special interest in atrial fibrillation (AF) as the most common heart rhythm disorder in clinical practice,[16] the recent discovery by members of our research group that neonatal rat atrial cardiomyocytes (AMs) possess a constitutively active acetylcholine-dependent K^+ current playing an important role in the development of AF[17] and the relatively low cell yields obtained from enzymatically dissociated neonatal rat atria, AMs were chosen as starting material. These cells were transduced with a single lentiviral vector (LV) allowing myocyte-restricted doxycycline (dox)/tetracycline-dependent LT expression followed by their clonal expansion in the presence of dox. The resulting monoclonal cell lines were characterized by cell proliferation assays, reverse transcription-quantitative polymerase chain reaction (RT-qPCR) analysis, phase-contrast, and immunofluorescence microscopy (IFM), western blotting, optical voltage mapping, and patch-clamp. The response of the cells to cardiac ion channel inhibitors, and their ability to integrate with pAMs were also investigated. Altogether, our data show that we have generated cardiomyocyte lines that (i) outperform all existing lines of cardiac muscle cells in terms of cardiomyogenic differentiation ability, (ii) have great potential as models for fundamental and applied cardiac research, and (iii) depending on the specific application, may provide easy-to-use and cost-effective alternatives for PSC-CMCs and for cardiomyocytes freshly isolated from animals.

Methods

Detailed methods are available in Supplementary material online.

Animal experiments

All animal experiments were approved by the Animal Experiments Committee of Leiden University Medical Center (LUMC) and conformed to the Guide for the Care and Use of Laboratory National Animals as stated by the US Institutes of Health.

Cardiac cell culture

Neonatal rat cardiomyocytes were isolated and cultured essentially as described.[18]

LV production

LV particles were produced using a previously published method.[18] The molecular structure of the shuttle plasmid used for the production of the LT-encoding LV is depicted in *Figure 1A*.

Molecular analyses

The primer pairs used for transcriptome analysis by RT-qPCR are shown in Supplementary material online, *Table S1*.

Details about the antibodies used for western blotting and immunostaining of formaldehyde-fixed cells are presented in Supplementary material online, *Table S2*.

Apoptosis was studied using Alexa Fluor-568-conjugated annexin V.

Electrophysiological studies

Optical voltage mapping using 4-(2-(6-(dibutylamino)-2-naphthalenyl) ethenyl)-1-(3-sulfopropyl)pyridinium hydroxide inner salt (di-4-ANEPPS) as fluorescent voltage indicator was performed essentially as described previously.[22] A detailed description of the whole-cell patch-clamp studies can be found in the Supplementary material online.

Statistical analyses

Data were derived from a specified number (*N*) of observations from three different cell cultures. Unless otherwise stated, data were expressed as mean ± standard deviation (SD), and SDs were represented by error bars. All data were analysed with the nested analysis of variance (ANOVA) test using the Real Statistics Resource Pack software (release 5.1, copyright 2013–2017, Charles Zaiontz, www.real-statistics.com). For comparisons involving >2 experimental groups, this test was followed by Bonferroni *post hoc* analysis. Results were considered statistically significant at *P*-values <0.05. Statistical significance was expressed as follows: $*P < 0.05$, $**P < 0.01$, $***P < 0.001$, $****P < 0.0001$.

Results

Conditional immortalization of AMs

Low-density cardiomyocyte-enriched cultures of primary cells isolated from the atria of 2-day-old Wistar rats were transduced with LV particles containing a dox-inducible LT expression unit based on the monopartite lentiviral Tet-on system developed by Szulc *et al.*[23] LT expression in this LV system was driven by the strong hybrid striated muscle-specific MHCK7 promoter[19] (*Figure 1A*) to minimize the likelihood of inadvertently immortalizing the ±12% non-cardiomyocytes present in the primary atrial cell cultures[17] (data not shown).

In the presence of dox, cells started to divide forming clearly discernible colonies at 1–3 weeks post-transduction (*Figure 1B*). Nine of >80 cell clones were randomly selected for testing the dox dependency of their proliferation ability. Cells of all nine clones were actively dividing in

the presence of dox and stopped doing so in its absence. To investigate whether these clones contained excitable cells, confluent monolayers were established, maintained in dox-free culture medium for 9 days and examined by optical voltage mapping. Following 1-Hz electrical stimulation, seven of the nine clones produced excitatory waves spreading from the pacing electrode to the opposite site of the culture dishes. Of these seven clones, clone no. 5 showed the shortest action potential (AP) duration (APD) and highest conduction velocity (CV) and was therefore picked for further investigation. Western blot analysis and IFM showed expression of LT in this clone to be tightly and effectively controlled by dox (*Figure 1C–E*).

Comparison of the light microscopic morphology of the conditionally immortalized AMs (iAMs) with those of primary AMs (pAMs) revealed that the surface area of proliferating iAMs did not significantly differ from that of pAMs at culture day 1 (*Figure 2A* and *E*). Also, in near-confluent monolayers, iAMs that were kept for 9 days in dox-free medium closely resembled pAMs at culture day 9 in both size and appearance (*Figure 2A*).

In the presence of dox, 72.2 ± 8.1% of iAMs stained positive for the proliferation marker Ki-67, which percentage dramatically decreased upon dox removal (*Figure 2B* and *F*). Consistently, in the presence of dox, iAMs proliferated with an average doubling time of 38 h, whereas under differentiation conditions (i.e. in the absence of dox), the cell number slightly decreased with time (*Figure 2G*). As expected, in primary atrial cell cultures, the percentage of α-actinin^{+} cells expressing Ki-67 was very low indicating that the large majority of proliferating Ki-67^{+} cells in these cultures are non-cardiomyocytes (*Figure 2C* and *F*). Probing iAM cultures with fluorescently labelled annexin V for the presence of surface-exposed phosphatidylserine as marker of apoptosis revealed low signals in proliferating cultures, which slightly increased under differentiation conditions (*Figure 2D* and *H*) but did not noticeably differ from those in 9-day-old pAM cultures (*Figure 2D* and *H*).

Cardiomyogenic differentiation potential of iAMs

The expression of cardiac marker genes in proliferating and differentiating iAM cultures was assessed by RT-qPCR analysis and compared with that of pAMs and of primary neonatal rat ventricular cardiomyocytes (pVMs) at culture day 9. Previous experience has shown that at this particular time point, the primary cardiomyocytes are optimally adapted to the *in vitro* environment and still in an advanced state of differentiation.[17,18,22,24,25] Expression of the *Nkx2.5*, *Gata4* and *Mef2c* genes, which encode early cardiac transcriptional regulators, was higher in proliferating (i.e. Day 0) iAMs than in pAMs and pVMs and rapidly increased soon after dox removal (*Figure 3A*). Expression of the sarcomeric protein-encoding *Actn2* and *Myh6* genes, on the other hand, was lower in Day 0 iAMs than in pAMs and pVMs. Transcription of these genes also showed a rapid increase under differentiation conditions to very similar levels as in pAMs and pVMs (*Figure 3A*).

To study myofibrillogenesis, cells were immunostained for sarcomeric α-actinin (*Figure 3B*). At the immortalized stage, α-actinin expression in iAMs was low and in most cells the protein was diffusely spread throughout the cytoplasm. However, in a few cells, α-actinin showed a punctate staining pattern with the protein clustering in spherical or short elongated structures. At Day 3 of differentiation, α-actinin formed longer structures with a dot-like appearance reminiscent of immature myofibrils. Myofibril assembly nearly reached completion at Day 6 after dox removal, with most of the α-actinin displaying the Z-line staining pattern typical of cardiomyocytes. At the later stages of differentiation (i.e. at Days 9 and 12 after dox removal), myofibrils underwent further maturation resulting in cells with highly organized sarcomeres.

After dox removal, mRNA levels of the atrial natriuretic peptide (ANP)-encoding *Nppa* gene, the atrial essential myosin light chain-encoding *Myl4* gene and the atrial regulatory myosin light chain (i.e. Mlc2a)-encoding *Myl7* gene were moderately (*Myl4*) to strongly (*Nppa* and *Myl7*) upregulated in iAMs (*Figure 3C*). Moreover, neither in the absence nor in the presence of dox, iAMs expressed detectable amounts of transcripts encoding ventricular regulatory myosin light chain (i.e. Mlc2v; *Myl2* gene), ventricular essential myosin light chain (*Myl3* gene) or β-myosin heavy chain (*Myh7* gene; *Figure 3C*). The RNA samples of 9-day-old pAM cultures contained high amounts of 'atrial' mRNA while 'ventricular' transcripts were barely detectable in these samples (*Figure 3C*). For the RNA samples from the 9-day-old pVM cultures the opposite was true, i.e. they contained high amounts of *Myl2*, *Myl3*, and *Myh7* transcripts but hardly any *Nppa*, *Myl4*, or *Myl7* mRNA (*Figure 3C*). Collectively, these data indicate that iAMs reacquire properties of atrial rather than ventricular cardiomyocytes when cultured in dox-free medium (*Figure 3C*). Mlc2a immunostaining confirmed these findings and showed gradual incorporation of this protein into sarcomeres indiscernible from those in pAMs that had been cultured for 9 days (*Figure 3D*). iAMs started to exhibit spontaneous contractions from Day 6 of differentiation (Supplementary material online, *Movie S1*) demonstrating sarcomere functionality. The immunostainings for α-actinin and Mlc2a also revealed that the spontaneous differentiation of iAMs in the absence of dox is a highly synchronous event occurring in essentially all cells at approximately the same time.

Electrophysiological properties of iAMs

RT-qPCRs targeting genes encoding cardiac ion channels showed an increase in the mRNA levels of *Scn5a*/$Na_v1.5$, *Cacna1c*/$Ca_v1.2$, *Kcnj3*/$K_{ir}3.1$, *Kcnj5*/$K_{ir}3.4$, and *Kcnj11*/$K_{ir}6.2$ during the early stages of iAM differentiation, which, later in the differentiation process, dropped to approximately equal levels as in pAMs at culture day 9 (Supplementary material online, *Figure S1A–E*). A similar differentiation-dependent trend in expression levels was observed for *Kcnd3*/$K_v4.3$ and *Kcnh2*/$K_v11.1$ but in these cases transcript levels at the late stages of iAM differentiation were higher than those in Day 9 pAMs (Supplementary material online, *Figure S1F* and *G*). The iAMs did not express detectable amounts of *Kcnj2*/$K_{ir}2.1$ at any stage in the differentiation process in contrast to pAMs that had been cultured for 9 days (Supplementary material online, *Figure S1H*). However, *Kcnj2* expression in pAMs was much lower than in pVMs at culture day 9. Transcript levels of the pacemaker channel genes *Hcn2* and *Hcn4* showed dynamic changes during the cardiomyogenic differentiation of iAMs (Supplementary material online, *Figure S1I* and *J*). Proliferating iAMs expressed more *Hcn2* mRNA than pAMs at Day 9 of culture, but this difference largely disappeared following 12 days of cardiomyogenic differentiation of the iAMs. The *Hcn4* mRNA level in proliferating iAMs was lower than in pAMs at culture day 9 but showed a gradual increase during the first 9 days of iAM differentiation to suddenly drop afterwards. RT-qPCR analysis of *Ryr2* and *Atp2a2*/Serca2 transcripts showed an increase in the expression of these Ca^{2+}-handling protein genes early during iAM differentiation. From Day 3 of differentiation onwards, *Ryr2* and *Atp2a2* mRNA levels in iAMs remained constant and were very similar (*Ryr2*) or 2- to 3-fold higher (*Atp2a2*) than in pAMs at culture day 9 (Supplementary material online, *Figure S1K* and *L*).

Since spreading of APs through cardiac tissue critically depends on the presence of intercellular conduits, iAM cultures at different stages of differentiation were immunostained for the gap junction protein connexin

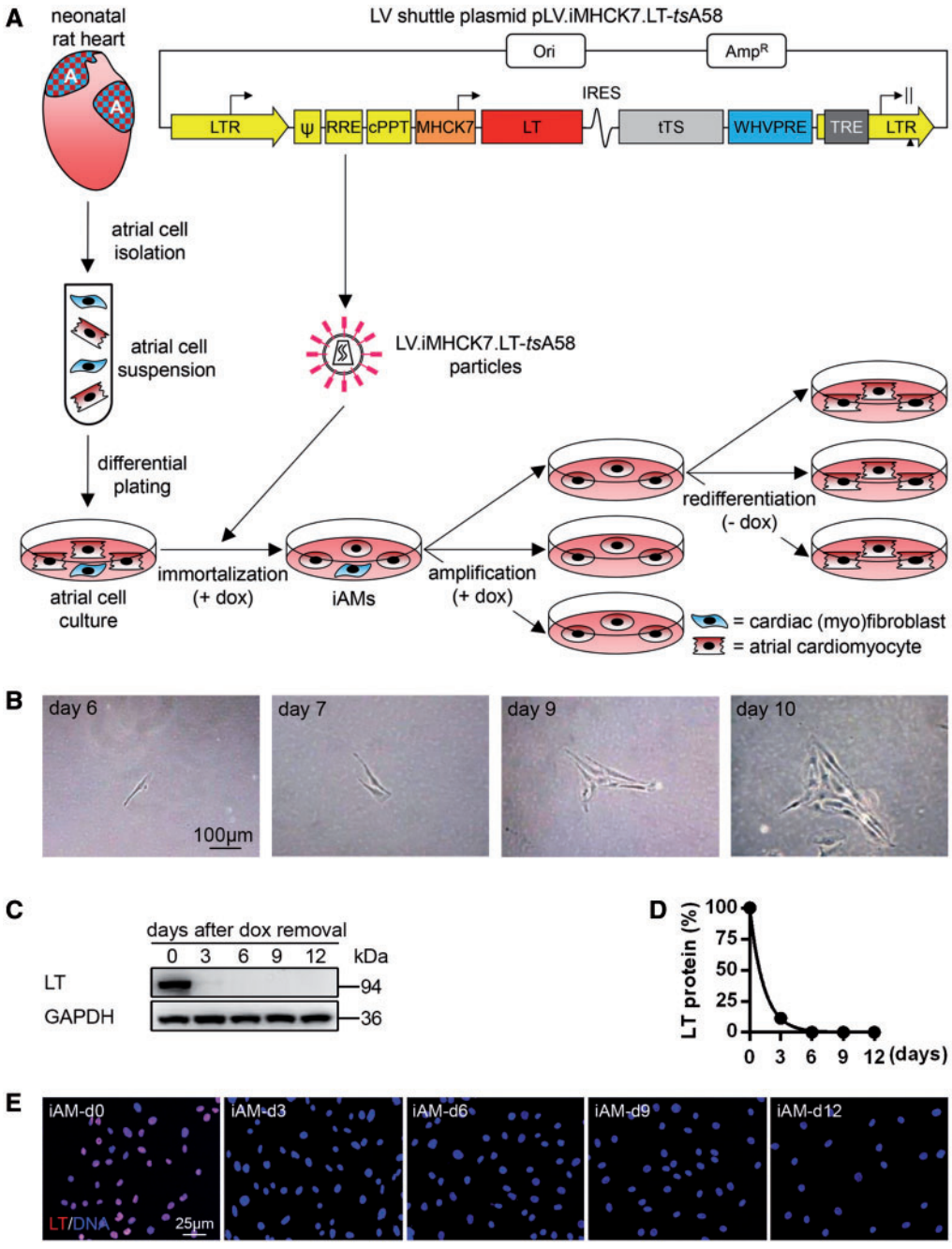

Figure 1 Conditional immortalization of pAMs. (*A*) Scheme of the procedure used for the reversible immortalization, amplification, and subsequent redifferentiation of pAMs. (*B*) Bright-field images of a single cell in an LT-transduced pAM culture showing dox-dependent clonal expansion. (*C–E*) Analysis by western blotting (*C, D*) and immunocytology (*E*) of LT protein expression in iAM cultures before (Day 0) and 3, 6, 9, and 12 days after dox removal. GAPDH, glyceraldehyde-3-phosphate dehydrogenase; A, atrium; Ori, bacterial origin of replication; Amp^R, *Escherichia coli* ß-lactamase gene; LTR, human immunodeficiency virus type 1 (HIV1) long terminal repeat; Ψ, HIV1 packaging signal; RRE, HIV1 Rev-responsive element; cPPT, HIV1 central polypurine tract and termination site; MHCK7, chimeric striated muscle-specific promoter;[19] LT, coding sequence of the temperature-sensitive mutant LT protein *ts*A58;[20] IRES, encephalomyocarditis virus internal ribosome entry site; tTS, coding sequence of the hybrid tetracycline-controlled transcriptional repressor TetR-KRAB;[21] WHVPRE, woodchuck hepatitis virus posttranscriptional regulatory element; TRE, tetracycline-responsive promoter element consisting of 7 repeats of a 19-nucleotide tetracycline operator (*tetO*) sequence.

43 (Cx43). As shown in *Figure 4A*, Cx43 was first observed in iAMs at 3 days after dox removal and its amounts gradually increased as the cells further differentiated. Initially, Cx43 was mainly detected in the perinuclear region (i.e. at the site of biosynthesis) but at Day 9 of differentiation, most Cx43 was found in punctate patterns at the interfaces between iAMs. To investigate the functionality of these gap junctional plaques, confluent monolayers of differentiated iAMs were subjected to 1-Hz electrical point stimulation, which caused the cells to contract at the

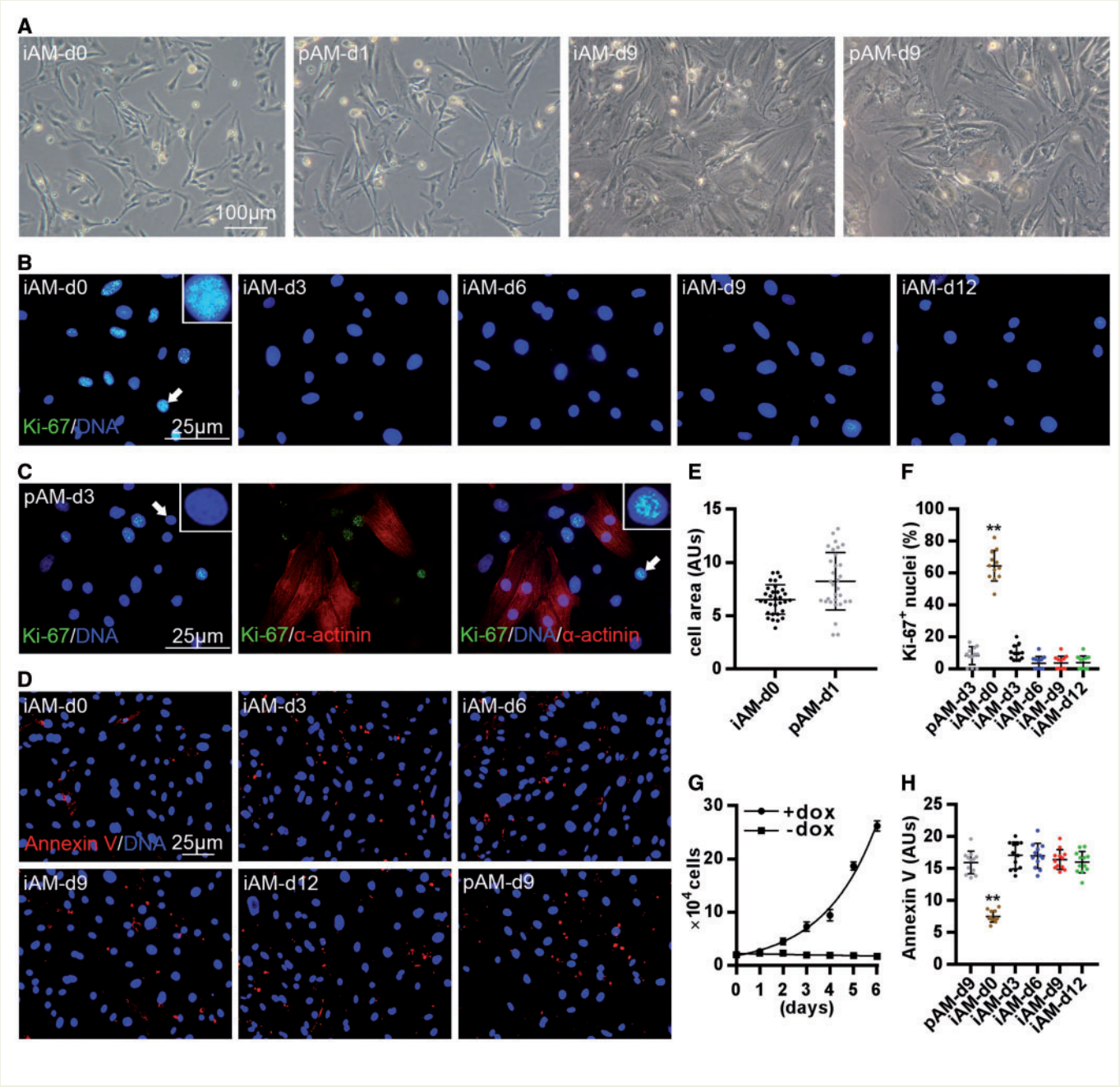

Figure 2 Morphology, proliferative activity, and apoptosis analysis of iAMs. (*A*) Bright-field images of proliferating iAMs (i.e. iAM-d0) and iAM-d9 and of pAMs at culture days 1 (pAM-d1) and 9 (pAM-d9). (*B*) Fluorescence images of proliferating iAMs and of iAMs at different days after dox removal immunostained for the proliferation marker Ki-67. The arrow is pointing at the nucleus shown at a higher magnification in the inset. (*C*) Fluoromicrograph of a 3-day-old pAM (pAM-d3) culture that was not subjected to mitomycin C treatment following double immunostaining for Ki-67 and sarcomeric α-actinin. The Ki-67^{+}/α-actinin^{-} cells observed in this culture mainly result from uninhibited proliferation of cardiac fibroblasts (data not shown). Arrows are pointing at the nuclei shown at a higher magnification in the insets. (*D*) Fluorescence images of proliferating iAMs, of iAMs at different days after dox removal and of a 9-day-old, mitomycin C-treated pAM (pAM-d9) culture labelled with Alexa Fluor-568-conjugated annexin V to assess externalization of phosphatidylserine as indicator of apoptosis. (*E*) Quantification of cell surface area of iAM-d0 and of pAM-d1. Data are presented as mean ± SD, $n = 30$ cells per experimental group, each consisting of three cell preparations. For statistical analysis, the nested ANOVA test was used. (*F*) Graph showing the percentage of Ki-67^{+} nuclei in proliferating iAM cultures, in iAM cultures at different days after dox removal, and among the cardiomyocytes (i.e. α-actinin^{+} cells) in pAM-d3 cultures. Data are presented as mean ± SD, $n = 12$ cell cultures per experimental group from three individual preparations. Statistics was done using the nested ANOVA test with Bonferroni *post hoc* correction. (*G*) Quantification of cell numbers in iAM cultures with or without dox. Data are presented as mean ± SD, $n = 3$. (*H*) Quantification of cell surface-bound annexin V in proliferating iAM cultures, in iAM cultures at different days after dox removal and in mitomycin C-treated pAM-d9 cultures. Data are presented as mean ± SD, $n = 12$ cell cultures per experimental group from three individual preparations. Statistics was done using the nested ANOVA test with Bonferroni *post hoc* correction. $^{**}P < 0.01$ vs. pAM cultures. AUs, arbitrary units.

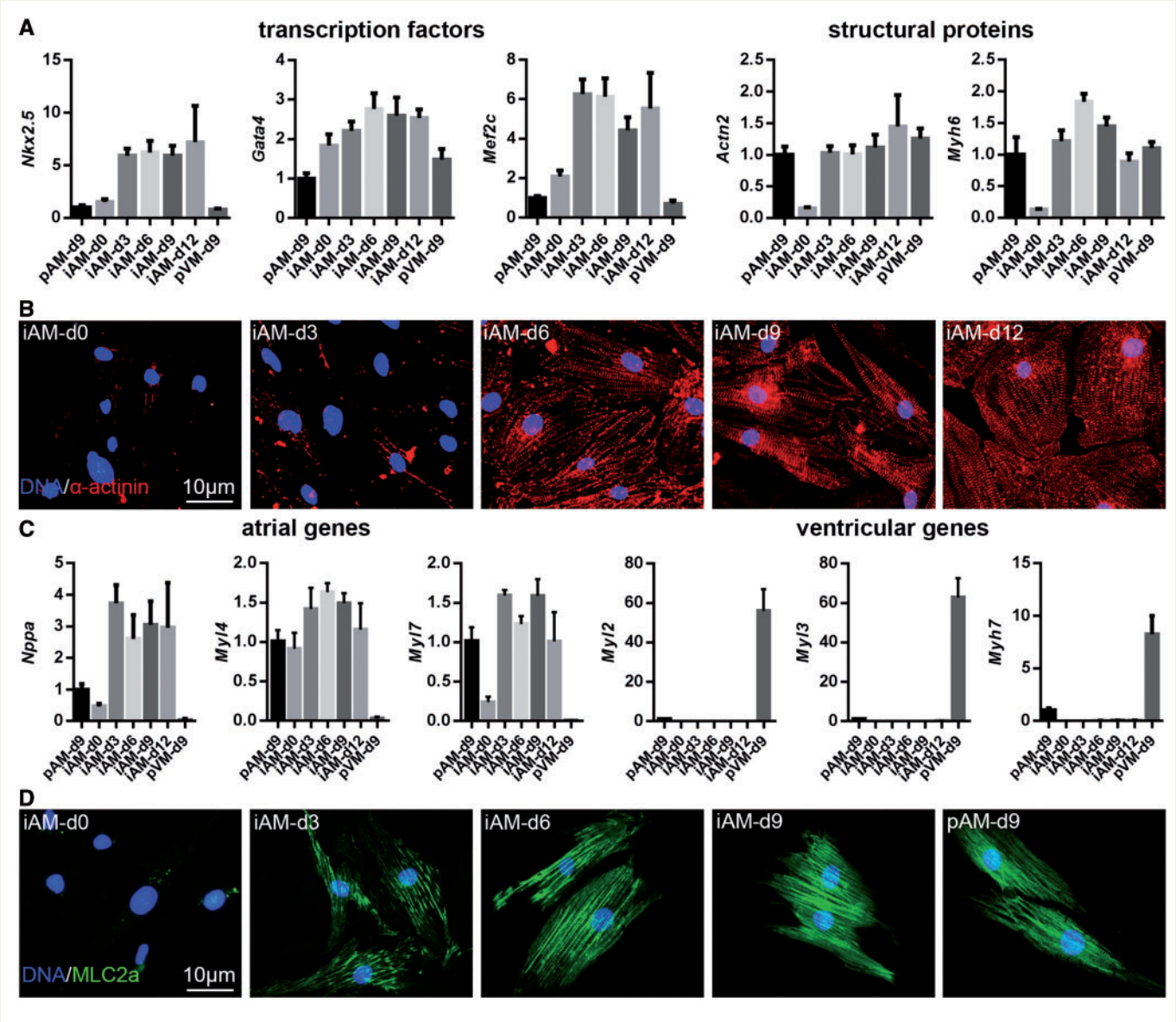

Figure 3 Cardiomyogenic differentiation potential of iAMs. (*A, C*) Analysis by RT-qPCR of the expression of the cardiac transcription factor genes *Nkx2.5*, *Gata4*, and *Mef2c*, the cardiac sarcomeric protein genes *Actn2* and *Myh6* (*A*), the 'atrial' genes *Nppa*, *Myl4*, and *Myl7* and the 'ventricular' genes *Myl2*, *Myl3*, and *Myh7* (*C*) in pAMs and pVMs at Day 9 of culture and in iAMs on the indicated days of differentiation. mRNA levels are expressed relative to those in 9-day-old pAM (pAM-d9) cultures, which were set at 1. Data are presented as mean ± SD, $n = 3$. The low abundance of 'atrial' transcripts in pAM samples is most likely due to the presence of some ventricular myocytes in these samples. Similarly, the pVM cultures may have contained low numbers of atrial myocytes. Alternatively, pAMs may express 'ventricular' genes at low levels and pVMs may display low-level expression of 'atrial' genes. (*B, D*) Fluorescence images of proliferating iAMs and of iAMs at different days after dox removal immunostained for sarcomeric α-actinin (red, *B*) or the atrial regulatory myosin light chain MLC2a (green, *D*). pAMs and pVMs at culture day 9 served as positive and negative control for the MLC2a immunostaining, respectively. Cell nuclei have been visualized by staining with Hoechst 33342 (blue).

pacing frequency (Supplementary material online, *Movie S2*). This result was corroborated by optical voltage mapping, which showed uniform radial spreading of excitatory waves from the site of electrical point stimulation in iAM cultures at Day 9 of differentiation (Supplementary material online, *Movie S3*). Additional optical voltage mapping experiments revealed a gradual increase in CV (*Figure 4B* and *D*; Supplementary material online, *Movie S3*) and decrease in APD (*Figure 4C, E*, and *F*) with ongoing iAM differentiation. As a matter of fact, CV and APD at 30% and 80% repolarization (APD_{30} and APD_{80}, respectively) did not significantly differ between iAM cultures at differentiation days 9 and 12 and 9-day-old pAM cultures. These data suggest that upon dox removal, iAMs differentiate into AMs with electrophysiological properties strongly resembling those of pAMs.

To investigate the ionic basis of the similar electrophysiological properties of pAMs and cardiomyogenically differentiated iAMs as measured by optical voltage, we conducted patch-clamp experiments on these cardiomyocytes. The resting membrane potentials (RMP) of pAMs and iAMs in monolayer culture did not significantly differ (-64.5 ± 1.2 mV,

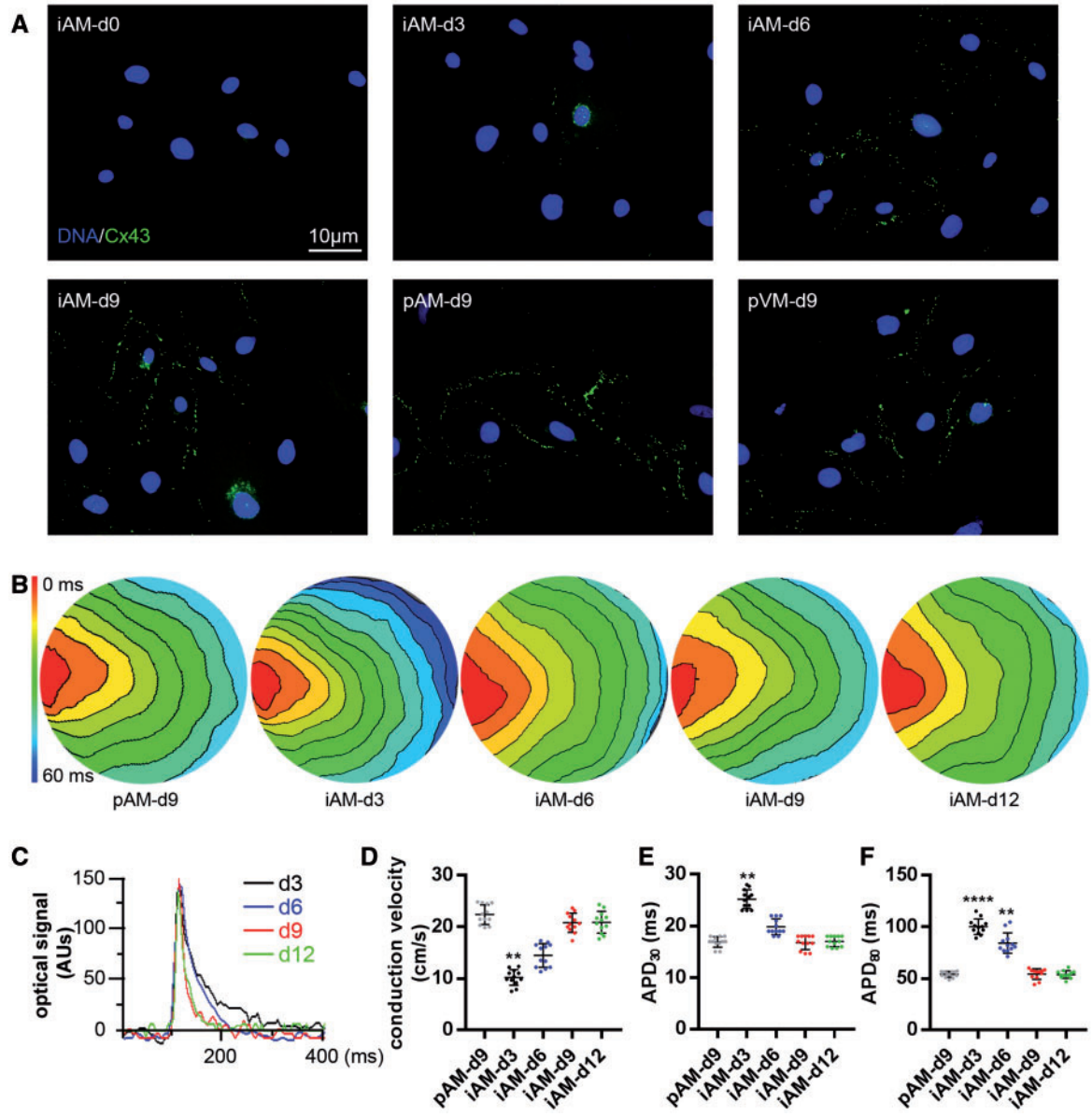

Figure 4 Electrophysiological properties of iAMs. (*A*) Fluorescence images of proliferating iAMs and of iAMs at different days after dox removal immunostained for Cx43 (green) showing its differentiation-dependent accumulation at the sarcolemma in gap junctional plaques. As positive controls for the Cx43 immunostaining, 9-day-old pAM and pVM cultures were included. Hoechst 33342 (blue) staining shows cell nuclei. (*B–F*) Optical voltage mapping of confluent iAM and 9-day-old pAM (pAM-d9) monolayers following 1-Hz electrical point stimulation. (*B, C*) Typical activation maps (*B*, isochrones are separated by 6 ms) and optical signal traces (*C*) of iAM cultures at different days after dox removal showing an increase in CV and a decrease in APD with advancing iAM differentiation. (*D–F*) Quantification of CV (*D*), APD_{30} (*E*), and APD_{80} (*F*) in pAM-d9 cultures and in iAM cultures at 3, 6, 9 and 12 days of differentiation. Data are presented as mean ± SD, $n = 12$ cell cultures per experimental group from 3 individual preparations. Statistics was done using the nested ANOVA test with Bonferroni *post hoc* correction. $^{**}P < 0.01$ and $^{****}P < 0.0001$ vs pAM-d9 cultures. AUs, arbitrary units.

$n = 15$ vs. -67.5 ± 1.6 mV, $n = 13$), while single-cell recordings showed pAMs to have a more negative RMP (-62.8 ± 1.8 mV, $n = 14$) than iAMs (-46.0 ± 1.9 mV, $n = 27$; Supplementary material online, *Figure S2A*). In spite of the measured difference in RMP between single pAMs and single iAMs, both cell types were excitable and produced APs with very similar characteristics under the same stimulation conditions (Supplementary material online, *Figure S2B* and *Table S3*). Of all the AP parameters assessed only the upstroke velocity and the overshoot were somewhat smaller for the iAMs in comparison to the pAMs (Supplementary material online, *Table S3*). In voltage-clamp experiments, we found that the main membrane current responsible for the excitability of both cell types is a fast voltage-activated transient Na^+ current (consistent with the expression of *Scn5a* in these cells, Supplementary material online, *Figure S1A*), which occurred in these cells as a dominant current component (see Supplementary material online, *Figure S2B, D*, and *E*). Although these patch-clamp results fit with the optical mapping data, we were puzzled

by the similar RMPs for pAM and iAM monolayers, given the undetectable *Kcnj2* expression in cardiomyogenically differentiated iAMs (Supplementary material online, *Figure S1H*) and the presumed difference in the inward rectifier current between pAMs and iAMs (I_{K1}; Supplementary material online, *Figure S2B*). This apparent discrepancy was resolved by showing, with the aid of ouabain, that the electrogenic Na^+/K^+ ATPase plays an important role in generating hyperpolarized RMPs in both pAMs and iAMs (Supplementary material online, *Figure S3*).

To investigate their ability to form a functional cardiac syncytium with pAMs, iAMs were labelled with enhanced green fluorescent protein (eGFP) by lentiviral transduction. Next, 1:1 co-cultures of pAMs treated at Day 1 of culture with mitomycin C, and eGFP-labelled iAMs were established and subsequently kept for 8 days in dox-free culture medium. The co-cultures were compared with iAM monocultures at Day 9 of differentiation and with 9-day-old, mitomycin C-treated pAM cultures (Supplementary material online, *Figure S4A*). Cx43 immunostaining of the co-cultures revealed the presence of gap junctions between iAMs and pAMs (Supplementary material online, *Figure S4B*). Optical voltage mapping showed uniform radial spreading of APs from the pacing electrode at roughly the same speed in all three culture types (Supplementary material online, *Figure S4C* and *D*) suggesting proper electrical integration of differentiated iAMs in co-cultures with pAMs.

Comparison of the electrophysiological properties of iAMs and HL-1 cells

The electrophysiological properties of iAM clone no. 5 were compared with those of the widely used HL-1 cell line, which was derived from the AT-1 mouse atrial myocyte tumour lineage.[11] To this end, confluent monolayers of iAMs at Day 9 of differentiation and optimally maintained confluent cultures of HL-1 cells were subjected to optical voltage mapping following 1-Hz pacing. The CV in the HL-1 cultures was ±20-fold lower than in the iAM cultures (*Figure 5A* and *B*; Supplementary material online, *Movie S3*), and HL-1 cells displayed greatly prolonged APs as compared to differentiated iAMs (*Figure 5C*) characterized by a very slow upstroke. These data clearly demonstrate that differentiated iAMs possess electrophysiological properties superior to those of HL-1 cells.

iAMs as *in vitro* model of AF

Our research group previously developed an *in vitro* model of AF based on high-frequency electrical stimulation of confluent pAM cultures. The resulting re-entrant circuits, or so-called rotors, could be terminated by prolonging APD of the pAMs using the $K_{ir}3.x$-specific inhibitor tertiapin.[17] To determine whether confluent cultures of iAMs at different stages of differentiation would display similar behaviour, they were burst paced in the absence or presence of 100 nM tertiapin. While rotors could be readily induced in iAM cultures from differentiation day 6 onwards (*Figure 6A-C*; Supplementary material online, *Movie S4*), re-entry could not be established in iAM cultures at Day 3 of differentiation (*Figure 6C*). Re-entry inducibility, the number of rotors per culture and rotor frequency increased with the time after dox removal (*Figure 6C–E*). After treatment with tertiapin, iAMs that had been cultured for 9 days without dox showed a strong increase in APD (*Figure 6F–H*). Moreover, in the presence of tertiapin it was no longer possible to induce re-entry in confluent monolayers of iAMs at Days 6, 9, or 12 of differentiation by burst pacing (*Figure 6C–F*). The fact that tertiapin treatment only slightly reduced the CV in confluent monolayers of iAMs at Day 9 of differentiation (from 20.5 to 19.8 cm/s; *Figure 6I*) suggests that Kir3.x channel activity is not the major determinant of iAM excitability at the monolayer level.

Discussion

Until now, all attempts to generate lines of cardiomyocytes that can give rise to cells with electrical and contractile properties approaching those of the starting material have failed. Indeed, all cardiomyocyte lines reported to date display large structural and functional deficits compared to the primary cardiomyocytes from which they were derived.[11,13,15,26] In this study, we have solved this problem and describe the generation of monoclonal lines of conditionally immortalized neonatal rat atrial myocytes with preserved cardiomyogenic differentiation capacity. This was accomplished by transducing pAMs with an LV directing myocyte-selective and dox-dependent expression of the SV40 LT antigen. Culturing of the resulting cells in medium with dox caused their rapid expansion, while in dox-free culture medium, the amplified cells spontaneously and synchronously differentiated into fully functional (i.e. excitable and contractile) AMs that were successfully used to develop a monolayer model of AF, for investigating the APD-prolonging effects of toxins (tertiapin, *Figure 6*). To provide our iAMs with a unique and easy-to-remember identifier, we have dubbed the progeny of iAM clone no. 5 the iAM-1 cell line.

Properties of iAMs

RT-qPCR analysis of iAMs in different stages of differentiation (*Figure 3* and Supplementary material online, *Figure S1*) showed a rapid increase in mRNA levels of cardiac transcription factors, ion channels, Ca^{2+}-handling proteins, and sarcomeric proteins shortly after dox removal. At later stages of differentiation, these mRNA levels generally either stayed fairly constant (as for the genes encoding cardiac transcription factors, sarcomeric, and Ca^{2+}-handling proteins and ANP) or declined again to the approximate mRNA levels of pAMs (*Scn5a*, *Cacna1c*, *Hcn2*, *Kcnj3*, *Kcnj11*) and/or proliferating iAMs (*Scn5a*, *Cacna1c*, *Kcnd3*, *Kcnh2*, *Kcnj3*). These findings are consistent with the notion that upon dox removal iAMs rapidly engage in a cardiomyogenic differentiation programme with the concomitant upregulation of genes needed to build a functional cardiomyocyte. To complement the RT-qPCR data, we recently initiated an RNA-seq study focussing on the transcriptomes of iAMs at different stages of cardiomyogenic differentiation and subsequent dedifferentiation. The results of this study will be presented elsewhere.

Following their differentiation in the absence of dox, iAMs acquire properties of atrial rather than ventricular myocytes as evinced by the high-level expression in differentiated iAMs of 'atrial' genes including *Nppa*, *Myl4*, *Myl7*, *Kcnj3*, and *Kcnj5*[17] and the lack of expression of the 'ventricular' *Myl2*, *Myl3*, and *Myh7* genes.[27] Moreover, following 1-Hz pacing, differentiated iAMs display rapid contractions that strongly resemble those of pAMs but are quite different from the slower contractions of pVMs (Supplementary material online, *Movie S2* and data not shown). Consistently, the average APD_{30} and APD_{80} of differentiated iAMs do not significantly differ from those of pAMs (*Figure 4E* and *F*, respectively; Supplementary material online, *Table S3*) but are much shorter than the average APD_{30} and APD_{80} of pVMs ($APD_{30} = 97.1 \pm 13.6$ ms and $APD_{80} = 242.8 \pm 25.2$ ms, $n = 17$). Collectively, these findings indicate that although LT expression results in the dedifferentiation and proliferation of AMs, the cells retain some kind of epigenetic memory causing them to spontaneously differentiate into atrial myocytes upon dox removal.

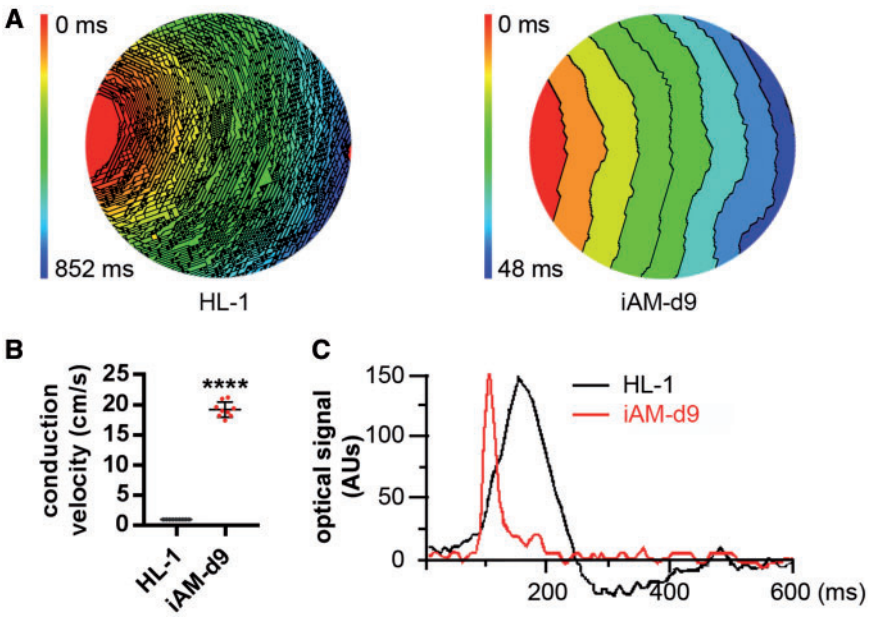

Figure 5 Comparison by optical voltage mapping and 1-Hz electrical point stimulation of the electrophysiological properties of confluent monolayers of iAMs at Day 9 of differentiation (iAM-d9) with those of HL-1 cells. Typical activation maps (*A*, 6-ms isochrone spacing) showing a much slower CV (*B*) and optical signal traces (*C*) showing a much longer APD for the HL-1 cells as compared to the iAM-d9. Data are presented as mean ± SD, $n = 9$ cell cultures per group from three individual preparations. For statistical analysis, the nested ANOVA test was used. ****$P < 0.001$. AUs, arbitrary units.

RMPs of iAMs and pAMs

pAM and iAM monolayers had similar RMPs (*Figure S2A*). Although RMP measurements of single cells are less reliable than those of cell clusters, because the voltage is measured from a high-resistance source ($R_m > 100$ MΩ) after establishing gigaseal, the RMPs of single pAMs and pAM monolayers did not significantly differ (*Figure S2A*). However, the RMP of single iAMs was significantly depolarized compared to that of iAM monolayers (*Figure S2A*). Further experiments as part of a dedicated patch-clamp study are needed to determine the precise cause for this difference, which may, however, relate to the lack of *Kcnj2* expression in cardiomyogenically differentiated iAMs (*Figure S1H*) together with technical difficulties to perform meaningful RMP measurements in neonatal/immature (atrial) cardiomyocytes due to their high plasma membrane resistance.[28,29]

Our finding that the electrogenic Na^+/K^+ ATPase plays an important role in the generation of the RMP of AMs is of particular interest, because it ensures a sufficiently negative RMP for the maintenance of excitability of iAMs in monolayer cultures, in the absence of *Kcnj2* expression. The importance of the Na^+/K^+ pump for establishing physiological Na^+ and K^+ gradients is widely recognized in the electrophysiology of adult cardiomyocytes. Decreased activity of the Na^+/K^+ pump under ischaemic conditions causes the loss of physiological K^+ and Na^+ gradients with consequent RMP depolarization and other effects favouring arrhythmogenesis.[30] However, as stated in many physiology textbooks, a direct contribution of the electrogenic action of the Na^+/K^+ pump to the RMP of adult cardiomyocytes is often considered as relatively small compared to the pump's indirect electrogenic effect, i.e. its ability to create transmembrane K^+ and Na^+ gradients. This may be understood by considering the Na^+/K^+ pumps in the plasma membrane as a low conductance pathway with a negative reversal potential determined by their ATP-driven action.[31,32] This implies that the direct electrogenic effects of pump currents will, at the same current densities, be more prominent in high-resistance (~1 GΩ) cardiomyocytes like the AMs than in lower-resistance (~100 MΩ) cardiomyocytes like adult rat ventricular cardiomyocytes.[33] Possibly, no/low expression of inward rectifier K^+ channels in iAMs and an important role for the Na^+/K^+ ATPase activity in setting the RMP is characteristic for young (atrial) myocytes or a sign of incomplete differentiation of these cells. Developmental increases in I_{K1} are not uncommon and have previously been reported for ventricular cardiomyocytes of various rodent species.[34]

Because of the dominance of voltage-activated Na^+ channels in the voltage-clamp recordings of both pAMs and iAMs, we ascribed the excitability of iAMs mainly to those channels. However, AMs also express, though at much lower levels, voltage-activated Ca^{2+} channels[35] (Supplementary material online, *Figure S1B*), which may be expected to contribute to pAM and iAM excitability. How these Ca^{2+} channels compare in their contribution to excitability in pAMs and iAMs deserves further experimental work. The same applies to the contributions of outward rectifier K^+ currents to the excitability of pAMs and iAMs, and to the realization of the RMP of single iAMs in general.

Possible applications of iAMs

Long-term culture of iAMs did not significantly reduce their proliferation rate in the presence of dox and the sarcomeric organization and contractile behaviour of iAMs from different passages at Day 9 of differentiation were indistinguishable (data not shown). Moreover, no progressive cell flattening, nuclear enlargement, development of senescence-associated heterochromatin foci, or other signs of senescence were observed during the first 55 population doublings of the cells. Assessment of the electrophysiological properties of confluent monolayers of

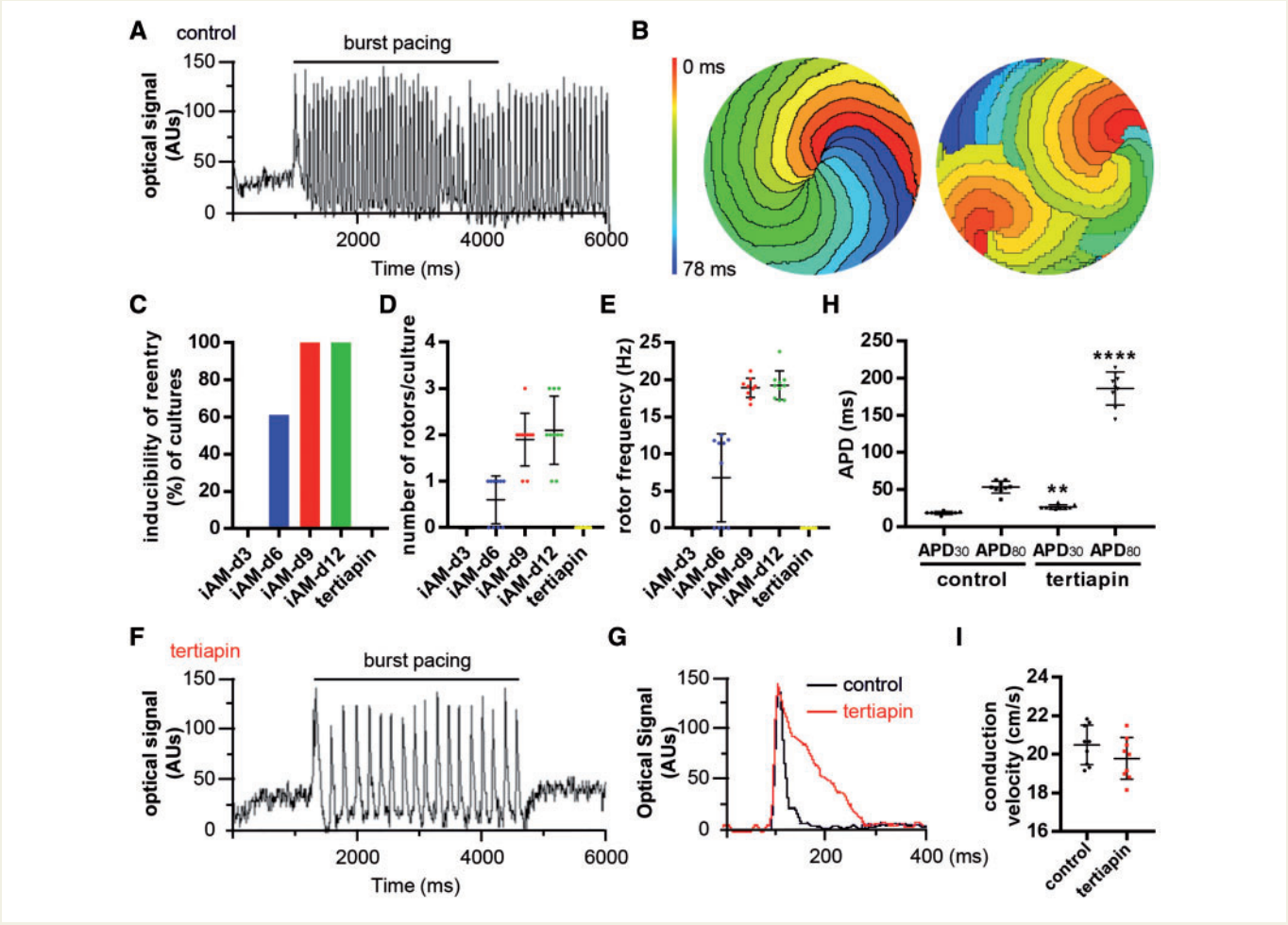

Figure 6 Suitability of iAMs as *in vitro* AF model assessed by optical voltage mapping. (*A*, *F*) Typical optical signal traces of mock- (*A*) and tertiapin (*F*)-treated iAMs at Day 9 of differentiation (iAM-d9) after high-frequency (10–50 Hz) electrical point stimulation. (*B*) Activation maps (6-ms isochrone spacing) of iAM-d9 cultures showing 1 (left) or 2 (right) re-entrant circuits. (*C*–*E*) Inducibility of re-entry (*C*), arrhythmia complexity (*D*) and quantification of rotor frequency (*E*) in iAM cultures at 3, 6, 9, and 12 days of differentiation. (*G*) Typical optical AP records of mock- (black) and tertiapin (red)-treated iAM-d9 following 1-Hz pacing. (*H* and *I*) Quantification of APD_{30}, APD_{80} (*H*) and CV (*I*) of mock- and tertiapin-treated iAM-d9. Data are presented as mean ± SD, in $n = 9$ cell cultures per experimental group from three individual preparations. Statistics was done using the nested ANOVA test with Bonferroni *post hoc* correction. $^{**}P < 0.01$ and $^{****}P < 0.0001$ vs. control cultures. AUs, arbitrary units.

differentiated iAMs by optical voltage mapping after 25, 40, and 55 population doublings revealed no significant differences in APD or CV (see Supplementary material online, *Figure S5*). Also, differentiated iAMs resume cell division following addition of dox to the culture medium and redifferentiate again into atrial myocytes following subsequent dox removal (data not shown). iAMs therefore provide a virtually unlimited supply of cardiomyocytes for fundamental research but may also prove very useful for: (i) the development of acquired disease models, (ii) identifying new therapeutic targets, (iii) screening of drugs and toxins, (iv) testing of new treatment modalities (e.g. gene and cell therapy), (v) production of biopharmaceuticals in bioreactors or encapsulated cell/tissue grafts, and (vi) the improvement of tissue engineering approaches. The recent rapid progress in genome editing technologies[36] will further expand the applicability of iAMs allowing them to be used as models for studying key aspects of inherited cardiomyopathies.

A highly attractive feature of the iAMs is that they spontaneously undergo cardiomyogenic differentiation in a synchronous and near quantitative manner in standard culture medium without dox. Contrarily, generation of cardiomyocytes from embryonic or induced PSCs requires their properly timed treatment with various cocktails of growth factors and small molecules.[5] This typically yields phenotypically heterogeneous populations of mostly immature cardiomyocytes contaminated with variable percentages of non-cardiomyocytes. Consequently, to obtain relatively pure populations of PSC-CMCs various different enrichment procedures have been developed.[37] Production of more or less homogeneous populations of cardiomyocytes from PSCs thus is a laborious, time-consuming, and costly endeavour as compared to the straightforward generation of atrial myocytes from iAMs. This may explain why there are very few reports on the use of PSC-CMCs to investigate cardiac arrhythmias in monolayer cultures by optical mapping,[8] while such experiments are easily performed with differentiated iAM monolayers (*Figures 4–6* and Supplementary material online, *Figures S3–S6*). Also, in contrast to PSC-CMCs, iAMs offer the possibility to study the molecular mechanisms involved in the transition

of a differentiated cardiomyocyte that is no longer able to undergo cytokinesis into an actively dividing cell. This is particularly relevant given the growing interest in the regeneration of mammalian hearts from within by stimulating cardiomyocytes surrounding the site(s) of cardiac injury to multiply themselves through cell division.[38,39] Current findings regarding the molecular changes accompanying the reactivation of cardiomyocyte proliferation should be interpreted with caution due to the presence of other cell types (e.g. cardiac fibroblasts and inflammatory cells) in most test materials. iAMs do not suffer from this drawback making them a potentially highly useful model system to study the mechanisms underlying cell cycle re-entry and progression of cardiomyocytes.

Optical voltage mapping of other clones of excitable iAMs yielded very similar results although not all of them reached the same maximum CV and minimum APD as clone no. 5 (e.g. clone no. 1 and no. 6; Supplementary material online, *Figure S6A–C* and *D–F*, respectively). An intriguing finding of this study is the difference in electrophysiological properties between the differentiated progeny of different iAM clones, which extends to iAM clones not presented in this study. The cause(s) of this heterogeneity is/are unclear given the fact that cardiomyogenically differentiated cells with a similarly high level of sarcomeric organization still differed in electrophysiological behaviour (data not shown). Therefore, besides a different propensity to mature, other factors might explain the electrophysiological differences between individual iAM clones. Different iAM clones may, for instance, be derived from different parts of the atria (e.g. left or right atrium, epi- or endocardial atrium) or represent different subtypes of atrial myocytes (i.e. nodal, bundle and working cells). Also, the number and location of the chromosomal insertion sites of the LV genomes and the cell's epigenetic status at the moment of immortalization may have contributed to the observed heterogeneity in electrophysiological properties between different iAM clones.

Although single-cell patch-clamp analysis can yield a wealth of information about the electrophysiological behaviour of individual cells and has been widely used to estimate the risk of drug-induced proarrhythmia, the technique does not directly assess proarrhythmic potential and is of limited use for studying arrhythmia mechanisms. Optical mapping, on the other hand, allows investigation of normal and disturbed cardiac electrical impulse propagation in a direct manner with high spatial and temporal resolution.[40,41] As demonstrated by the experiments described *in Figures 4–6* and Supplementary material online, *Figures S3–S6*, confluent iAM cultures are well-suited for optical mapping studies. In combination with their large proliferation capacity, this opens perspectives for developing high-throughput analyses based on the iAM lines and/or future lines of other cardiomyocytes generated with our conditional immortalization method.

Comparison between HL-1 and iAM-1 cells

Of all AM lines generated to date, the murine AM line HL-1 has the most differentiated phenotype and is therefore most widely used. Side-by-side comparison of the electrophysiological properties of confluent monolayers of differentiated iAM-1 cells and HL-1 cells by optical voltage mapping (*Figure 5* and Supplementary material online, *Movie S3*) showed an average CV for the HL-1 cultures of 1 cm/s, which is about 20-fold lower than that of differentiated iAM-1 cell cultures and in line with previous reports.[26] Since Ma *et al.*[42] reported a RMP of -77.7 ± 0.4 mV for HL-1 cells at an extracellular K^+ concentration of 4 mM, the low CV in confluent HL-1 cell monolayers does not seem to result from a high percentage of cardiac fast Na^+ channels being in an inactivated state. The large difference in CV between both cell types thus conceivably relates to the fact that confluent HL-1 monolayers are a blend of proliferating cells without cardiomyocyte functionality, which are electrically coupled to cells that phenotypically resemble embryonic atrial myocytes.[11] Conversely, in the iAM cultures at 9 days of differentiation virtually all cells are in a similar advanced stage of differentiation forming a highly conductive cardiac syncytium (*Figures 4* and *5*; Supplementary material online, *Figures S4–S6*). Gap junctional coupling between undifferentiated and differentiated cells may also explain the apparent discrepancy between the broad optical voltage traces of HL-1 cells in monolayer cultures vs. the short APDs recorded for single HL-1 cells following whole-cell current clamping.[26]

Conclusion

By employing a monopartite LV system allowing inducible expression of the SV40 LT antigen in cardiomyocytes, we have generated lines of iAMs with (functional) properties superior to those of all existing cardiomyocyte lines, none of which yields cells that approach the structural and functional maturity of dox-deprived iAMs. This is especially true for differentiated iAM-1 monolayers, which show homogeneous AP propagation at much higher speeds than obtained with other lines of cardiac muscle cells. The broad applicability of the iAMs was illustrated by their use (i) to study the cardiac ion channel-modulatory activity of toxins and drugs and (ii) as AF model. Since iAMs undergo a highly coordinated and precisely timed cardiomyogenic differentiation process, they might also be ideally suited to study specific aspects of cardiac muscle cell formation and maturation. Finally, because differentiation of iAMs into electrically and mechanically active cardiomyocytes that phenotypically resemble atrial myocytes of new-born rats occurs spontaneously (i.e. without the need for complex treatment regimens with expensive [bio]chemicals), iAMs may provide an easy-to-use and cost-effective system to address specific fundamental and applied cardiac research questions.

Supplementary material

Supplementary material is available at *Cardiovascular Research* online.

Acknowledgements

We thank Brian Bingen, Zeinab Neshati plus Iolanda Feola, Niels Harlaar, and Annemarie Kip from LUMC's Laboratory of Experimental Cardiology for their help with establishing AM cultures, LV production, generating movie files, and RT-qPCR experiments, respectively. We are indebted to Bianca Brundel and Deli Zhang (Department of Physiology, Institute for Cardiovascular Research, VU University Medical Center) for supplying HL-1 cells.

Conflict of interest: none declared.

Funding

This study received financial support from the Netherlands Heart Institute (ICIN grant 230.148-04 to A.A.F.d.V.), the Royal Netherlands Academy of Arts and Sciences (Chinese Exchange Programme grant 10CDP007 to A.A.F.d.V.), and Ammodo (to D.A.P. and A.A.F.d.V.). Additional support came from the research programme More Knowledge with Fewer Animals (MKMD) with project number 114022503 (to A.A.F.d.V.), which is (partly)

financed by the Netherlands Organisation for Health Research and Development (ZonMw) and the Dutch Society for the Replacement of Animal Testing (dsRAT) and from the Chinese Scholarship Council (to J.L.).

References

1. Hasenfuss G. Animal models of human cardiovascular disease, heart failure and hypertrophy. *Cardiovasc Res* 1998;**39**:60–76.
2. Robinson N, Souslian L, Gallegos RP, Rivard AL, Dalmasso AP, Bianco RW, *Animal models for cardiac research*. In: PA. Iaizzo (ed.). *Handbook of Cardiac Anatomy, Physiology, and Devices*. 3rd ed. Cham: Springer International Publishing; 2015. pp. 469–491.
3. Mitcheson JS, Hancox JC, Levi AJ. Cultured adult cardiac myocytes: future applications, culture methods, morphological and electrophysiological properties. *Cardiovasc Res* 1998;**39**:280–300.
4. Parameswaran S, Kumar S, Verma RS, Sharma RK. Cardiomyocyte culture - an update on the in vitro cardiovascular model and future challenges. *Can J Physiol Pharmacol* 2013;**91**:985–998.
5. Spater D, Hansson EM, Zangi L, Chien KR. How to make a cardiomyocyte. *Development* 2014;**141**:4418–4431.
6. Karakikes I, Ameen M, Termglinchan V, Wu JC. Human induced pluripotent stem cell-derived cardiomyocytes: insights into molecular, cellular, and functional phenotypes. *Circ Res* 2015;**117**:80–88.
7. Veerman CC, Kosmidis G, Mummery CL, Casini S, Verkerk AO, Bellin M. Immaturity of human stem-cell-derived cardiomyocytes in culture: fatal flaw or soluble problem? *Stem Cells Dev* 2015;**24**:1035–1052.
8. Herron TJ. Calcium and voltage mapping in hiPSC-CM monolayers. *Cell Calcium* 2016;**59**:84–90.
9. Steinhelper ME, Lanson NA Jr, Dresdner KP, Delcarpio JB, Wit AL, Claycomb WC, Field LJ. Proliferation in vivo and in culture of differentiated adult atrial cardiomyocytes from transgenic mice. *Am J Physiol* 1990;**259**:H1826–H1834.
10. Jahn L, Sadoshima J, Greene A, Parker C, Morgan KG, Izumo S. Conditional differentiation of heart- and smooth muscle-derived cells transformed by a temperature-sensitive mutant of SV40 T antigen. *J Cell Sci* 1996;**109** (Pt 2):397–407.
11. Claycomb WC, Lanson NA Jr, Stallworth BS, Egeland DB, Delcarpio JB, Bahinski A, Izzo NJ Jr, HL-1 cells: a cardiac muscle cell line that contracts and retains phenotypic characteristics of the adult cardiomyocyte. *Proc Natl Acad Sci USA* 1998;**95**:2979–2984.
12. Rybkin II, Markham DW, Yan Z, Bassel-Duby R, Williams RS, Olson EN. Conditional expression of SV40 T-antigen in mouse cardiomyocytes facilitates an inducible switch from proliferation to differentiation. *J Biol Chem* 2003;**278**:15927–15934.
13. Davidson MM, Nesti C, Palenzuela L, Walker WF, Hernandez E, Protas L, Hirano M, Isaac ND. Novel cell lines derived from adult human ventricular cardiomyocytes. *J Mol Cell Cardiol* 2005;**39**:133–147.
14. Goldman BI, Amin KM, Kubo H, Singhal A, Wurzel J. Human myocardial cell lines generated with SV40 temperature-sensitive mutant tsA58. *In Vitro Cell Dev Biol Anim* 2006;**42**:324–331.
15. Zhang Y, Nuglozeh E, Toure F, Schmidt AM, Vunjak-Novakovic G. Controllable expansion of primary cardiomyocytes by reversible immortalization. *Hum Gene Ther* 2009;**20**:1687–1696.
16. Lip GY, Fauchier L, Freedman SB, Van Gelder I, Natale A, Gianni C, Nattel S, Potpara T, Rienstra M, Tse HF, Lane DA. Atrial fibrillation. *Nat Rev Dis Primers* 2016;**2**:16016.
17. Bingen BO, Neshati Z, Askar SF, Kazbanov IV, Ypey DL, Panfilov AV, Schalij MJ, de Vries AA, Pijnappels DA. Atrium-specific Kir3.x determines inducibility, dynamics, and termination of fibrillation by regulating restitution-driven alternans. *Circulation* 2013;**128**:2732–2744.
18. Feola I, Teplenin A, de Vries AA, Pijnappels DA. Optogenetic engineering of atrial cardiomyocytes. *Methods Mol Biol* 2016;**1408**:319–331.
19. Salva MZ, Himeda CL, Tai PW, Nishiuchi E, Gregorevic P, Allen JM, Finn EE, Nguyen QG, Blankinship MJ, Meuse L, Chamberlain JS, Hauschka SD. Design of tissue-specific regulatory cassettes for high-level rAAV-mediated expression in skeletal and cardiac muscle. *Mol Ther* 2007;**15**:320–329.
20. Loeber G, Tevethia MJ, Schwedes JF, Tegtmeyer P. Temperature-sensitive mutants identify crucial structural regions of simian virus 40 large T antigen. *J Virol* 1989;**63**:4426–4430.
21. Deuschle U, Meyer WK, Thiesen HJ. Tetracycline-reversible silencing of eukaryotic promoters. *Mol Cell Biol* 1995;**15**:1907–1914.
22. Bingen BO, Engels MC, Schalij MJ, Jangsangthong W, Neshati Z, Feola I, Ypey DL, Askar SF, Panfilov AV, Pijnappels DA, de Vries AA. Light-induced termination of spiral wave arrhythmias by optogenetic engineering of atrial cardiomyocytes. *Cardiovasc Res* 2014;**104**:194–205.
23. Szulc J, Wiznerowicz M, Sauvain MO, Trono D, Aebischer P. A versatile tool for conditional gene expression and knockdown. *Nat Methods* 2006;**3**:109–116.
24. Majumder R, Engels MC, de Vries AA, Panfilov AV, Pijnappels DA. Islands of spatially discordant APD alternans underlie arrhythmogenesis by promoting electrotonic dyssynchrony in models of fibrotic rat ventricular myocardium. *Sci Rep* 2016;**6**:24334.
25. Yu Z, Liu J, van Veldhoven JP, Ap IJ, Schalij MJ, Pijnappels DA, Heitman LH, de Vries AA. Allosteric modulation of Kv11.1 (hERG) channels protects against drug-induced ventricular arrhythmias. *Circ Arrhythm Electrophysiol* 2016;**9**:e003439.
26. Dias P, Desplantez T, El-Harasis MA, Chowdhury RA, Ullrich ND, Cabestrero de Diego A, Peters NS, Severs NJ, MacLeod KT, Dupont E. Characterisation of connexin expression and electrophysiological properties in stable clones of the HL-1 myocyte cell line. *PLoS One* 2014;**9**:e90266.
27. Lompre AM, Nadal-Ginard B, Mahdavi V. Expression of the cardiac ventricular alpha- and beta-myosin heavy chain genes is developmentally and hormonally regulated. *J Biol Chem* 1984;**259**:6437–6446.
28. Horváth A, Lemoine MD, Löser A, Mannhardt I, Flenner F, Uzun AU, Neuber C, Breckwoldt K, Hansen A, Girdauskas E, Reichenspurner H, Willems S, Jost N, Wettwer E, Eschenhagen T, Christ T. Low resting membrane potential and low inward rectifier potassium currents are not inherent features of hiPSC-derived cardiomyocytes. *Stem Cell Rep* 2018;**10**:822–833.
29. Dawodu AA, Monti F, Iwashiro K, Schiariti M, Chiavarelli R, Puddu PE. The shape of human atrial action potential accounts for different frequency-related changes in vitro. *Int J Cardiol* 1996;**54**:237–249.
30. Carmeliet E. Cardiac ionic currents and acute ischemia: from channels to arrhythmias. *Physiol Rev* 1999;**79**:917–1017.
31. Gadsby DC, Nakao M. Steady-state current-voltage relationship of the Na/K pump in guinea pig ventricular myocytes. *J Gen Physiol* 1989;**94**:511–537.
32. Läuger P. *Electrogenic ion pumps*. Sinauer, 1991.
33. Ypey DL, van Meerwijk WPM, Umar S, Pijnappels DA, Schalij MJ, van der Laarse A. Depolarization-induced automaticity in rat ventricular cardiomyocytes is based on the gating properties of L-type calcium and slow Kv channels. *Eur Biophys J* 2013;**42**:241–255.
34. Itoh H. Electrophysiological simulation of developmental changes in action potentials of cardiomyocytes. In: SNV Arjunan, PK Dhar, M, Tomita (eds). *E-Cell System: Basic Concepts and Applications*. New York: Springer; 2013. pp. 75-88.
35. Avila G, Medina IM, Jiménez E, Elizondo G, Aguilar CI. Transforming growth factor-β1 decreases cardiac muscle L-type Ca^{2+} current and charge movement by acting on the $Ca_v1.2$ mRNA. *Am J Physiol Heart Circ Physiol* 2007;**292**:H622–H631.
36. Maggio I, Goncalves MA. Genome editing at the crossroads of delivery, specificity, and fidelity. *Trends Biotechnol* 2015;**33**:280–291.
37. Schwach V, Passier R. Generation and purification of human stem cell-derived cardiomyocytes. *Differentiation* 2016;**91**:126–138.
38. Foglia MJ, Poss KD. Building and re-building the heart by cardiomyocyte proliferation. *Development* 2016;**143**:729–740.
39. Uygur A, Lee RT. Mechanisms of cardiac regeneration. *Dev Cell* 2016;**36**:362–374.
40. Herron TJ, Lee P, Jalife J. Optical imaging of voltage and calcium in cardiac cells & tissues. *Circ Res* 2012;**110**:609–623.
41. Himel HDIV, Bub G, Lakireddy P, El-Sherif N. Optical imaging of arrhythmias in the cardiomyocyte monolayer. *Heart Rhythm* 2012;**9**:2077–2082.
42. Ma L, Zhang X, Chen H. TWIK-1 two-pore domain potassium channels change ion selectivity and conduct inward leak sodium currents in hypokalemia. *Sci Signal* 2011;**4**:ra37.